PP2A/B56 and GSK3/Ras suppress PKB activity during *Dictyostelium* chemotaxis

Marbelys Rodriguez Pino[a], Boris Castillo[a], Bohye Kim[a], and Lou W. Kim[a,b,c]
[a]Department of Biological Sciences, [b]Biochemistry PhD Program, and [c]Biomolecular Sciences Institutes, Florida International University, Miami, FL 33199

ABSTRACT **We have previously shown that the *Dictyostelium* protein phosphatase 2A regulatory subunit B56, encoded by *psrA*, modulates *Dictyostelium* cell differentiation through negatively affecting glycogen synthase kinase 3 (GSK3) function. Our follow-up research uncovered that B56 preferentially associated with GDP forms of RasC and RasD, but not with RasG in vitro, and *psrA*$^-$ cells displayed inefficient activation of multiple Ras species, decreased random motility, and inefficient chemotaxis toward cAMP and folic acid gradient. Surprisingly, *psrA*$^-$ cells displayed aberrantly high basal and poststimulus phosphorylation of *Dictyostelium* protein kinase B (PKB) kinase family member PKBR1 and PKB substrates. Expression of constitutively active Ras mutants or inhibition of GSK3 in *psrA*$^-$ cells increased activities of both PKBR1 and PKBA, but only the PKBR1 activity was increased in wild-type cells under the equivalent conditions, indicating that either B56- or GSK3-mediated suppressive mechanism is sufficient to maintain low PKBA activity, but both mechanisms are necessary for suppressing PKBR1. Finally, cells lacking RasD or RasC displayed normal PKBR1 regulation under GSK3-inhibiting conditions, indicating that RasC or RasD proteins are essential for GSK3-mediated PKBR1 inhibition. In summary, B56 constitutes inhibitory circuits for PKBA and PKBR1 and thus heavily affects *Dictyostelium* chemotaxis.**

Monitoring Editor
Carole Parent
National Institutes of Health

Received: Jun 18, 2014
Revised: Sep 8, 2015
Accepted: Sep 21, 2015

INTRODUCTION

Motility is a process that involves multiple signaling pathways designed to allow cells to receive extracellular signals and orchestrate intracellular signaling network, which in turn affects cytoskeleton-based cell motility machinery. During the aggregation stage of *Dictyostelium*, the extracellular cAMP activates G protein–coupled receptors, resulting in the dissociation of heterotrimeric G proteins into Gα and Gβγ subunits (Janetopoulos *et al.*, 2001; Xu *et al.*, 2005; reviewed in Swaney *et al.*, 2010). The Gβγ subunits have been suggested to activate multiple downstream signaling components, including small GTPases such as RasC, RasG, RasB, and Rap1. Activation of RasG is critical for local accumulation of phosphatidylinositol-3,4,5,-triphosphate (PIP3) and, consequently, localizing pleckstrin homology (PH) domain–containing proteins such as PKBA, CRAC, and PhdA from the cytosol to the leading edge, where extensive remodeling of cytoskeleton is mediated by phosphorylation of protein kinase B (PKB) substrates (Funamoto *et al.*, 2002; Iijima and Devreotes, 2002). RasC, in parallel with RasG, mediates activation of TorC2 and subsequent activation of PKBA and PKBR1 at the leading edge (Insall *et al.*, 1996; Lee *et al.*, 2005; Kae *et al.*, 2007; Kamimura *et al.*, 2008). RasB and Rap1 proteins are known to mediate chemoattractant-mediated suppression of myosin II through activating myosin heavy chain kinase A (MHCKA) (Kortholt *et al.*, 2006; Jeon *et al.*, 2007a,b; Mondal *et al.*, 2008). Rear contraction and adhesion to the matrix are shown to be dependent on the cGAMP-mediated activation of myosin II.

An important family of kinases that modulates cytoskeletal remodeling in *Dictyostelium* is the AGC family of kinases, Akt/PKBA and protein kinase B–related 1 (PKBR1). In response to cAMP stimulation, RasG-dependent phosphatidylinositol 3 kinase (PI3K) activation transiently produces PIP3, to which PKBA translocalizes with its PH domain. Once at the plasma membrane, PKBA becomes phosphorylated by phosphoinositide-dependent kinase A (PdkA) and the Tor complex 2 (TorC2) in the activation loop (AL) site and

This article was published online ahead of print in MBoC in Press (http://www.molbiolcell.org/cgi/doi/10.1091/mbc.E14-06-1130) on September 30, 2015.
Address correspondence to: Lou W. Kim (kiml@fiu.edu).

Abbreviations used: AL, activation loop; dnGSK3, dominant-negative glycogen synthase kinase 3; GSK3, glycogen synthase kinase 3; HM, hydrophobic motif; PdkA, phosphoinositide-dependent kinase A; PH, pleckstrin homology; PKB, protein kinase B; PKBR1, protein kinase B–related 1; PP2A, protein phosphatase 2A; RBD, Ras binding domain; TorC2, Tor complex 2.

the hydrophobic motif (HM) site, respectively (Meili *et al.*, 1999; Kamimura *et al.*, 2008; Kamimura and Devreotes, 2010; Cai *et al.*, 2010; Liao *et al.*, 2010). In contrast to PKBA, PKBR1 does not have the PH domain; instead, PKBR1 is permanently anchored at the membrane through a myristoylation site present on its N-terminus (Meili *et al.*, 2000). PKBR1, however, also becomes activated upon cAMP stimulation by phosphorylation in both the AL site by PdkA and in the HM site by TorC2 (Kamimura *et al.*, 2008, 2010; Cai *et al.*, 2010; Liao *et al.*, 2010). Despite this difference in their subcellular localization mechanisms, both PKBA and PKBR1 activation involves Pdk1- and TorC2-mediated phosphorylation. The mechanism of cAMP-mediated activation of TorC2 is well characterized, but that of Pdk1 is still to be fully uncovered.

Previous studies also showed that Ras proteins have both distinct and overlapping functions (Khosla *et al.*, 2000), and cells lacking RasG, but not RasC, express higher level of RasD (Bolourani *et al.*, 2010). Considering that *rasG*$^{-}$/*C*$^{-}$ cells express lower level of RasD compared with the *rasG*$^{-}$ cells, RasC is likely contributing to the up-regulation of RasD expression (Bolourani *et al.*, 2010).

Cells overexpressing constitutively active RasD(G12T) mutant displayed exaggerated expression of the prestalk A cell marker *ecmA*. Interestingly, cells expressing dominant-negative glycogen synthase kinase 3 (dnGSK3 [K84M, K85M]; Kim *et al.*, 2002; Lee *et al.*, 2008) or treated with the GSK3 inhibitor LiCl also showed similarly enhanced *ecmA* expression. It was thus suggested that Ras and GSK3 may interact in the context of prestalk cell differentiation (Weeks, 2000). Previous studies showed that *gsk3*$^{-}$ cells are not only defective in cell differentiation but also highly compromised in chemotaxis (Teo *et al.*, 2010; Kim *et al.*, 2011). Potential mechanisms behind the *gsk3*$^{-}$ chemotaxis phenotype include biased localization of PI3K toward the plasma membrane, high poststimulus Ras activity, and compromised PKBR1-inhibiting signal through Ras effector Daydreamer (Teo *et al.*, 2010; Kölsh *et al.*, 2012; Sun *et al.*, 2013). There exist, however, contrasting data for the effect of GSK3 ablation on PKBR1 and PKBA activity (Teo *et al.*, 2010; Kölsh *et al.*, 2012; Sun *et al.*, 2013). Thus, to provide additional insight into the role of GSK3 for the PKB regulation, we analyzed the effects of GSK3 on PKBs by expressing dnGSK3 or treating cells with LiCl.

Previous studies demonstrated that a B56 subunit inhibits Akt in *Caenorhabditis elegans* and in differentiated 3T3-L1 adipocyte cells (Padmanabhan *et al.*, 2009). Another line of studies also showed that protein phosphatase 2A (PP2A)/B56 could dephosphorylate phospho-ERK2 and phospho-Akt through scaffolding protein IEX-1, which was induced by active Erk2. IEX-1 functions as a scaffolding platform for ERK2 and PP2A/B56, and thus facilitates Erk2-mediated phosphorylation of B56 that stimulates B56 dissociation from the PP2A core dimer, which then no longer inhibits Erk2 and Akt (Letourneux *et al.*, 2006; Rocher *et al.*, 2007). Furthermore, studies using mammalian cells demonstrated that insulin-mediated activation of PDK and mTorC2 not only activates Akt, but also stimulates the formation of the PP2A/B56 holoenzyme complex, which in turn dephosphorylates phospho-Akt (Rodgers *et al.*, 2011). These studies indicate that B56-mediated Akt inhibition is widely conserved among eukaryotes. In this report, we show the PP2A regulatory subunit, B56, and the glycogen synthase kinase 3 (GSK3) negatively regulate PKB activation in *Dictyostelium* cells, providing a novel insight into PKB regulation.

RESULTS

B56 preferentially associated with inactive RasC and RasD in vitro

As B56 is a known regulatory subunit for PP2A, the recombinant *Dictyostelium* B56 protein associated with PP2A catalytic subunit. In addition, the GST-B56 pull-down complex also included a small GTPase Ras (Figure 1A). To uncover the identity of Ras species that can associate with GST-B56, the whole-cell lysates from cells expressing Flag-tagged RasG, RasD, and RasC were incubated with GST-B56 and the Ras proteins associated with B56 were analyzed by Western blot. GST-B56 associated with Flag-RasD and Flag-RasC, but not with Flag-RasG (Figure 1, B and C).

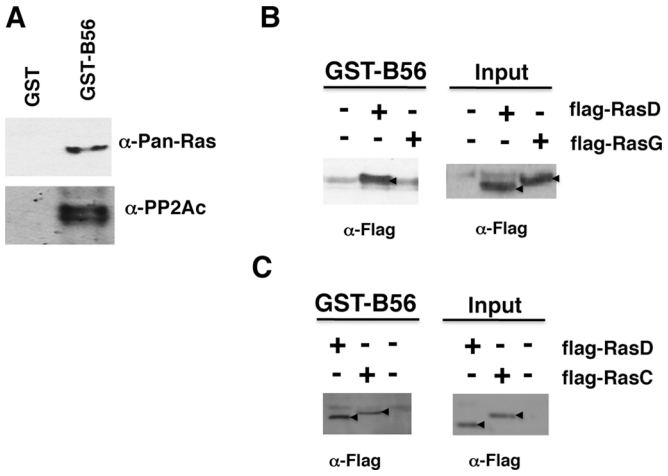

FIGURE 1: B56 associated with Ras proteins in addition to PP2A catalytic subunit. (A) GST-B56 pull-down assay uncovered that *Dictyostelium* B56 can associate with Ras proteins and PP2A catalytic subunit. Neither PP2Ac nor Ras proteins were detected from GST control. (B) GST-B56 exhibited stronger association with Flag-RasD over Flag-RasG (marked with arrowheads). (C) Flag-RasC is another *Dictyostelium* Ras species that showed strong association with B56. Bands corresponding to Flag-RasD and Flag-RasC are marked with arrowheads. Representative data from three independent experiments are shown.

Given that the GST pull-down assays were performed with whole-cell lysates from unstimulated cells, in which the majority of the Ras proteins are inactive, it is likely that GDP-Ras proteins were included in the GST-B56 pull-down complex. To determine whether activated GTP-Ras proteins can also associate with B56, the Flag-Ras–containing lysates were treated with GTP-γ-S and then incubated with GST-B56, GST-Raf1–Ras binding domain (RBD), or GST-Byr2-RBD proteins. On incubation with GTP-γ-S, more Ras proteins associated with GST-RBD, but significantly fewer Ras proteins were included in the GST-B56 pull-down complex (Figure 2A). In addition, the recombinant proteins of constitutively active or dominant-negative mutant Flag-RasD and Flag-RasC were generated in *Escherichia coli* and were incubated with either GST-B56 or GST-RBD proteins. Consistent with GTP-γ-S experiments, the constitutively active Ras mutants displayed less binding to GST-B56, and the dominant-negative Ras mutants exhibited enhanced association with GST-B56 (Figure 2B).

The discovery that B56 can associate not only with RasD but also with RasC suggests that B56 is likely to be involved in the regulation of cell motility in addition to cell differentiation, which was previously reported (Lee *et al.*, 2008). Considering that GDP-Ras bound more tightly to B56 and that certain RasGefs such as RasGefQ prefer GDP-Ras (Mondal *et al.*, 2008), it is plausible that B56 may facilitate recruiting GDP-Ras to specific RasGef proteins.

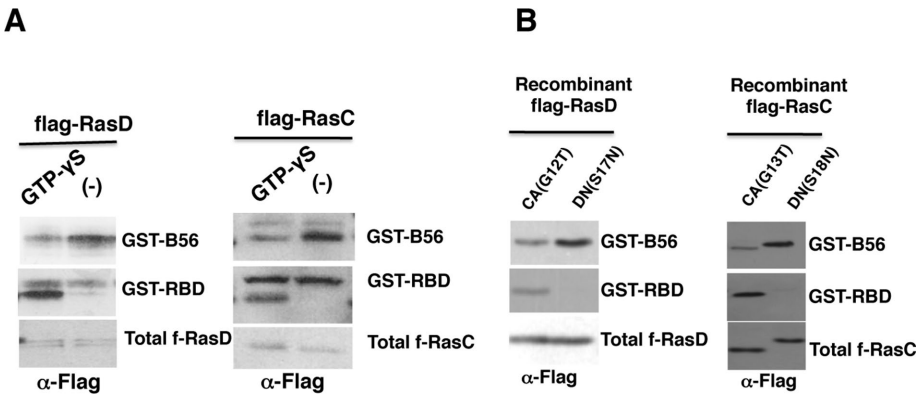

FIGURE 2: The GDP-bound or inactive form of Ras preferably associated with B56. (A) Stimulation of whole-cell lysate with GTPγS increased Flag-RasD and Flag-RasC binding to GST-Raf1-RBD, but exhibited the opposite pattern with GST-B56. (B) Dominant-negative forms of recombinant Flag-RasD(S17N) and Flag-RasC(S18N) displayed strong binding to GST-B56 but not the constitutive active forms of Flag-RasD(G12T) and Flag-RasC(G13T). The constitutive active Ras mutants showed stronger binding to GST-Raf1-RBD as expected. The dominant-negative mutants showed much weaker binding to GST-Raf1-RBD. Representative data from three independent experiments are shown.

psrA⁻ cells exhibited compromised cAMP-induced Ras activation

Dictyostelium cells possess 11 different Ras species and two Rap proteins (http://dictybase.org; Chattwood *et al.*, 2014); among those, RasG and RasC have been shown to be critical regulators of cellular migration (Kortholt and van Haastert, 2008). RasG and RasC regulate recruitment and activation of several downstream effectors involved in cellular motility, including PI3K and TorC2. Axenically grown cells lacking both RasG and RasC exhibited severely compromised motility and cAMP-mediated signaling (Kortholt and van Haastert, 2008; Charest *et al.*, 2010).

To determine whether B56 also affects Ras activity, active Ras levels were measured using the RBD of mammalian Raf1 XE "Ras Binding Domain of mammalian Raf1" ($GST\text{-}RBD_{Raf1\ XE\ "GST\text{-}RBDRaf1"}$) or the RBD of *Schizosaccharomyces pombe* Byr2 XE "Ras Binding Domain from *Schizosaccharomyces pombe* Byr2" ($GST\text{-}RBD_{Byr2\ XE\ "GST\text{-}RBDByr2"}$). The peak Ras activities were detected in wild-type cells at 5 s after cAMP stimulation, which decreased thereafter, but *psrA*⁻ cells exhibited significantly reduced Ras activation in response to cAMP stimulation (Figure 3, A and B).

psrA⁻ cells were defective in random and directional motility

psrA⁻ cells stimulated with pulsatile cAMP exhibited an average velocity of random motility that is 50% reduced compared with *Wt* cells (Figure 4A). When the cell motility of *psrA*⁻ cells was examined in the presence of an external cAMP gradient (10 μM cAMP), *psrA*⁻ cells moved more slowly compared with *Wt* cells, exhibiting an average velocity reduced by 60% compared with *Wt* cells (Figure 4B). Furthermore, *psrA*⁻ cells displayed significantly compromised chemotaxis; *psrA*⁻ cells exhibited an ~50% reduced chemotaxis index compared with that of wild-type cells. These results suggest that B56 is part of a regulatory network controlling both random and directional motility of aggregation-competent *Dictyostelium*. To further corroborate that PP2A/B56 is an essential part of the cell motility regulatory network, axenically grown vegetative-stage wild-type and *psrA*⁻ cells were challenged with a micropipette filled with folic acid (0.1 mM). As shown in Figure 4C, *psrA*⁻ cells exhibited statistically significant compromise in directional migration toward the folic acid gradient, indicating that B56 is a critical factor for chemotaxis machinery. *psrA*⁻ cells also exhibited an ~50% reduction in speed.

PKBR1 activity and PKBs substrate phosphorylation were aberrantly high in *psrA*⁻ cells

Considering that *psrA*⁻ cells have generally low Ras activity, we hypothesized that PKBA and PKBR1 activation may also be compromised in *psrA*⁻ cells. For examination of PKBA and PKBR1 activation, aggregation-competent cells were stimulated with cAMP and the phosphorylation levels of PKBA and PKBR1 at the activation loop (AL) site were examined as previously described (Cai *et al.*, 2010). On cAMP stimulation, wild-type cells exhibited phosphorylation at the AL site in PKBR1 and PKBA between 15 and 30 s, which decreased back to the basal level at 60 s after cAMP stimulation. In contrast, a higher basal level of phosphorylated PKBR1, but not PKBA, was observed in *psrA*⁻ cells compared with *Wt* cells (Figure 5A). Furthermore, *psrA*⁻ cells displayed higher basal phosphorylation of T470 of the HM of PKBR1 ($p < 0.05$; Figure 5B). Total protein levels stained with Coomassie were used as a loading control.

To further investigate the effect of B56 in PKB regulation, we examined the phosphorylation of putative PKB substrates containing the motif R-x-R-x-x-S/T-x-x (x denotes a random amino acid) in *psrA*⁻ as previously described (Kamimura *et al.*, 2008; Cai *et al.*, 2010). As expected, there were higher levels of phosphorylation of previously identified PKB substrates in *psrA*⁻ cells compared with *Wt* cells (Figure 5C). In addition, there were several novel phospho-PKB substrates (marked with asterisks) that seemed to be unique to *psrA*⁻ cells, the identification of which requires further investigation.

To determine whether *psrA*⁻ cells overproduce PKBR1, thus permitting Pdk1 and TorC2 to more easily phosphorylate PKBR1, we compared the levels of *PKBR1* messages in aggregation-competent wild-type and *psrA*⁻ cells by reverse transcription PCR (RT-PCR) (Figure 5D). The levels of *PKBR1* messages in wild-type and *psrA*⁻ cells were comparable, as were the *lg7* messages, the internal control. Thus B56 affects PKBR1 activity without altering its expression level.

Introducing constitutively active RasD increased PKBA and PKBR1 activities in *psrA*⁻ cells

Considering that RasD exerted a negative effect on chemotaxis toward cAMP (Khosla *et al.*, 2000), we hypothesized that RasD may mediate PKBR1 adaptation and that compromised RasD activity in *psrA*⁻ cells might therefore have caused increased PKBR1 phosphorylation. To that end, RasD activity in *psrA*⁻ cells was determined as shown in Figure 6A: the Flag-RasD activities were significantly lower in *psrA*⁻ cells ($*p < 0.05$), which is consistent with the generally diminished Ras activity in *psrA*⁻ cells.

To determine whether the low RasD activity in *psrA*⁻ cells caused a high level of PKB phosphorylation, we expressed constitutively active RasD mutant in wild-type and *psrA*⁻ cells (Figure 6, B and C). Contrary to expectations, RasD(G12T) expressing wild-type and *psrA*⁻ cells displayed even higher levels of active PKBR1 compared with their control cells (*Wt* cells, $*p < 0.05$; *psrA*⁻ cells, $**p < 0.01$), while RasC(G13T)-expressing *psrA*⁻ cells displayed enhanced levels

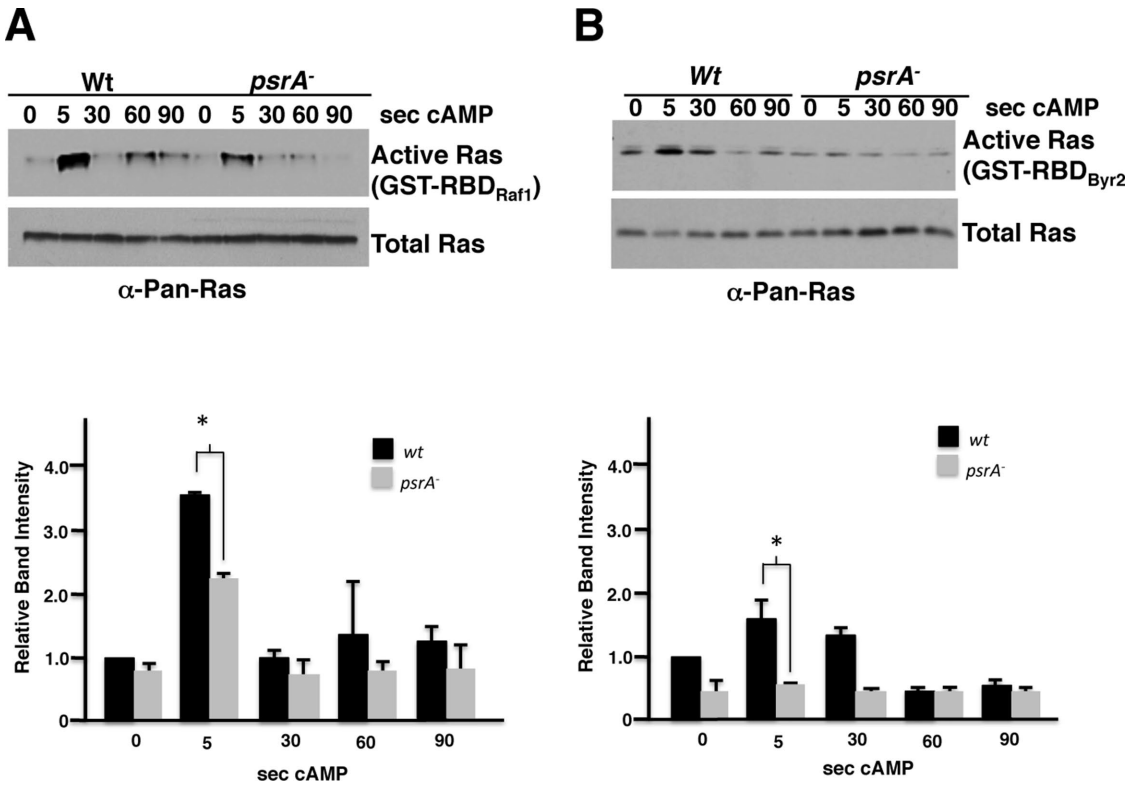

FIGURE 3: The chemoattractant cAMP-induced Ras activation was compromised in *psrA*⁻ cells. (A) *psrA*⁻ cells exhibited reduced amplitude of Raf1-RBD binding activity (presumably GTP-RasD and GTP-RasG) in response to cAMP stimulation compared with *Wt* cells. The Raf1-RBD binding activity of *psrA*⁻ cells at 5 s after cAMP stimulation is only ~60% compared with that of wild-type cells (three independent experiments; *, $p < 0.05$). (B) *psrA*⁻ cells also showed similar reduction (~30%) in Byr2-RBD binding activity (presumably GTP-RasC) in response to cAMP stimulation compared with *Wt* cells (three independent experiments, *t* test; *, $p < 0.05$). Error bars represent SD.

of PKBR1 activity as expected (Cai *et al.*, 2010) (Figure 6D). Thus compromised Ras activation of *psrA*⁻ cells is unlikely to be the cause of the high PKBR1 activity.

Interestingly the RasD(G12T) expression in *psrA*⁻ cells, but not in wild-type cells, induced a significantly higher level of PKBA activation in response to cAMP (**$p < 0.01$; Figure 6C), suggesting that B56 is necessary to maintain low PKBA activity against RasD signaling. RasC(G13T) expression in *psrA*⁻ cells showed increased AL site phosphorylation of PKBR1, but not of PKBA (Figure 6D). A previous study reported that RasD forms a complex that includes PKBA (Bandala-Sanchez *et al.*, 2006). Thus it is plausible that a chemoattractant-signaling cascade may not only activate RasD but may also induce dissociation of B56/PP2A from PKBA containing RasD and thus insulate B56/PP2A from PKBA.

Inhibition of GSK3 increased PKBA and PKBR1 activities in *psrA*⁻ cells

As mentioned earlier, several studies showed that GSK3 affects PKBs (Teo *et al.*, 2010; Kölsh *et al.*, 2012; Sun *et al.*, 2013). Considering the existence of conflicting reports using *gsk3*⁻ cells, we analyzed wild-type and *psrA*⁻ cells expressing dnGSK3 or treated with LiCl. Wild-type cells expressing dnGSK3 showed significantly elevated basal and poststimulus levels of PKBR1 phosphorylation (Figure 7A), and *psrA*⁻ cells expressing dnGSK3 exhibited even higher levels of basal and poststimulus PKBR1 phosphorylation and significantly increased PKBA activation in response to cAMP stimulation (Figure 7B). Increased total GSK3 level of dnGSK3-expressing cells compared with the parental cells are shown as a control (Figure 7, A and B).

Consistent with the phenotype of dnGSK3-expressing cells, LiCl-treated wild-type cells displayed a statistically significant increase in the basal PKBR1 level (**$p < 0.01$) as well as cAMP-induced PKBR1 activation (Figure 8A). *psrA*⁻ cells pretreated with LiCl also exhibited higher basal and cAMP-induced PKBR1 phosphorylation (Figure 8B). *gsk3*⁻ cells, in contrast to the cells expressing dnGSK3 or treated with LiCl, showed no PKBR1 phosphorylation regardless of LiCl treatment (Figure 8C), indicating that the effect of LiCl is GSK3 dependent. Thus the high GSK3 activity in *psrA*⁻ cells (Lee *et al.*, 2008) is unlikely to be the main cause for the high PKBR1 activity in *psrA*⁻ cells. We also noticed that, unlike dnGSK3-expressing *psrA*⁻ cells, *psrA*⁻ cells treated with LiCl demonstrated no increase in PKBA. Although LiCl can clearly inhibit GSK3, it can also block cAMP-dependent PIP3 generation and thus insulate PKBA activation (King *et al.*, 2009). The molecular nature of LiCl-mediated inhibition of cAMP-induced PKBA activation is currently unclear, but in any case, PP2A/B56 is not necessary for the LiCl effect.

Ras is essential for dnGSK3- and LiCl-mediated regulation of PKBR1 activation

Recent reports suggested that GSK3 affects Ras adaptation (Kölsh *et al.*, 2012; Sun *et al.*, 2013). Considering that Ras proteins are abnormally regulated in *gsk3*⁻ cells and they are PKBR1 activators, it is plausible that GSK3 inhibits PKBR1 through Ras proteins. To determine whether RasD is necessary for GSK3-mediated PKBR1 regulation, we overexpressed dnGSK3 in *rasD*⁻ cells. When the PKBR1 activation was examined in *rasD*⁻ cells overexpressing dnGKS3, no such drastic increase in PKBR1 phosphorylation as observed in

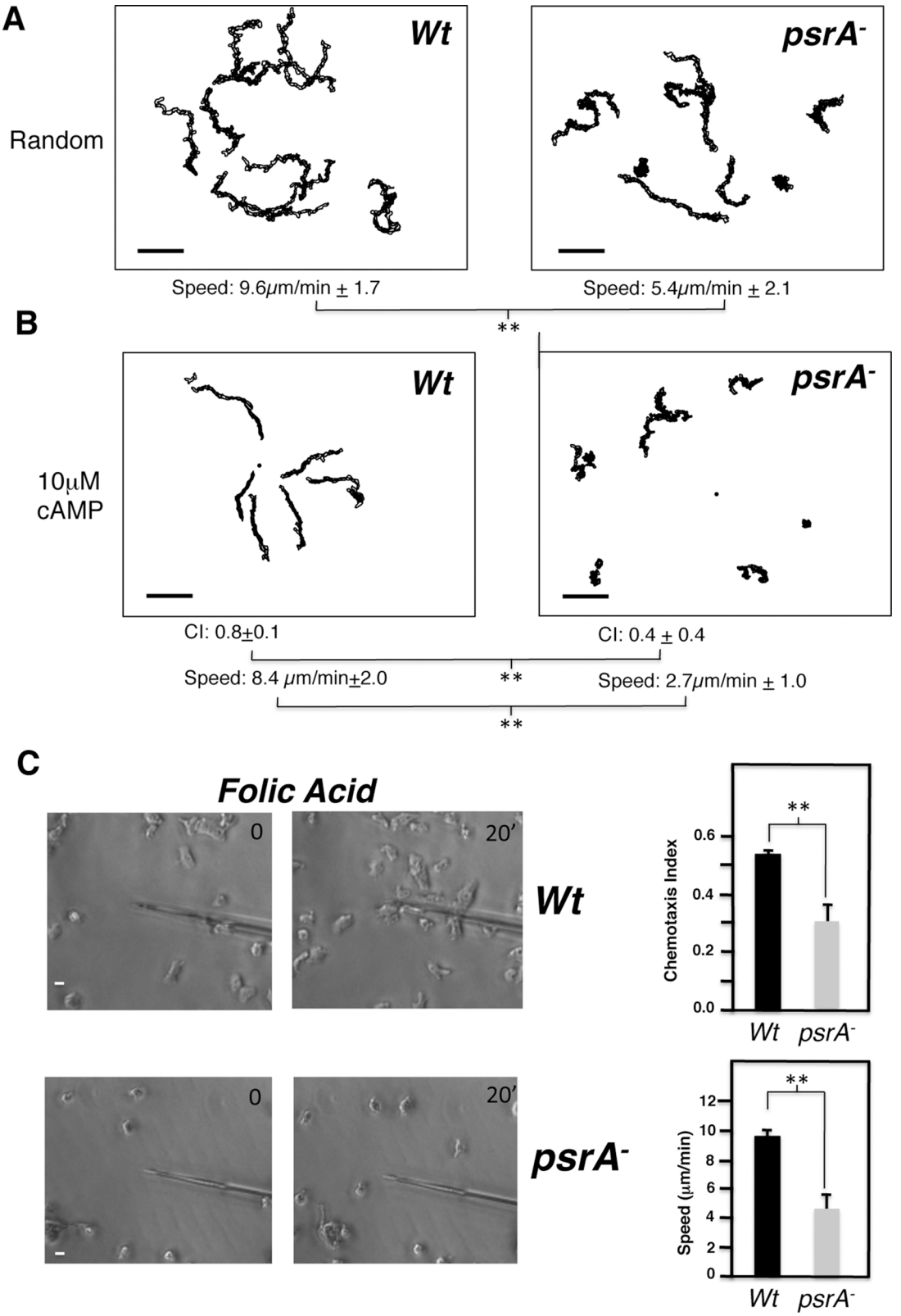

FIGURE 4: *psrA*⁻ cells displayed compromised random motility and chemotaxis. (A and B) Aggregation-competent wild-type cells after 4 h of pulsatile cAMP stimulation displayed robust random (~10 μm/min) and directional (8 μm/min) motility toward cAMP gradient (10 μM cAMP). In contrast, *psrA*⁻ cells exhibited only ~50% of random and ~40% of directional motility compared with wild-type cells. The chemotaxis index of *psrA*⁻ cells toward cAMP gradient was ~50% of that for wild type. Error bars represent SD. All three *p* values were < 0.01. (C) Axenically grown vegetative wild-type and *psrA*⁻ cells were challenged with 0.1 mM folic acid, and their movements were analyzed for 20 min. The chemotaxis index and speed of movement of *psrA*⁻ cells under folic acid gradient were reduced to ~60% and ~50% of the wild-type level, respectively. Error bars represent SE of the mean. All *p* values were < 0.01.

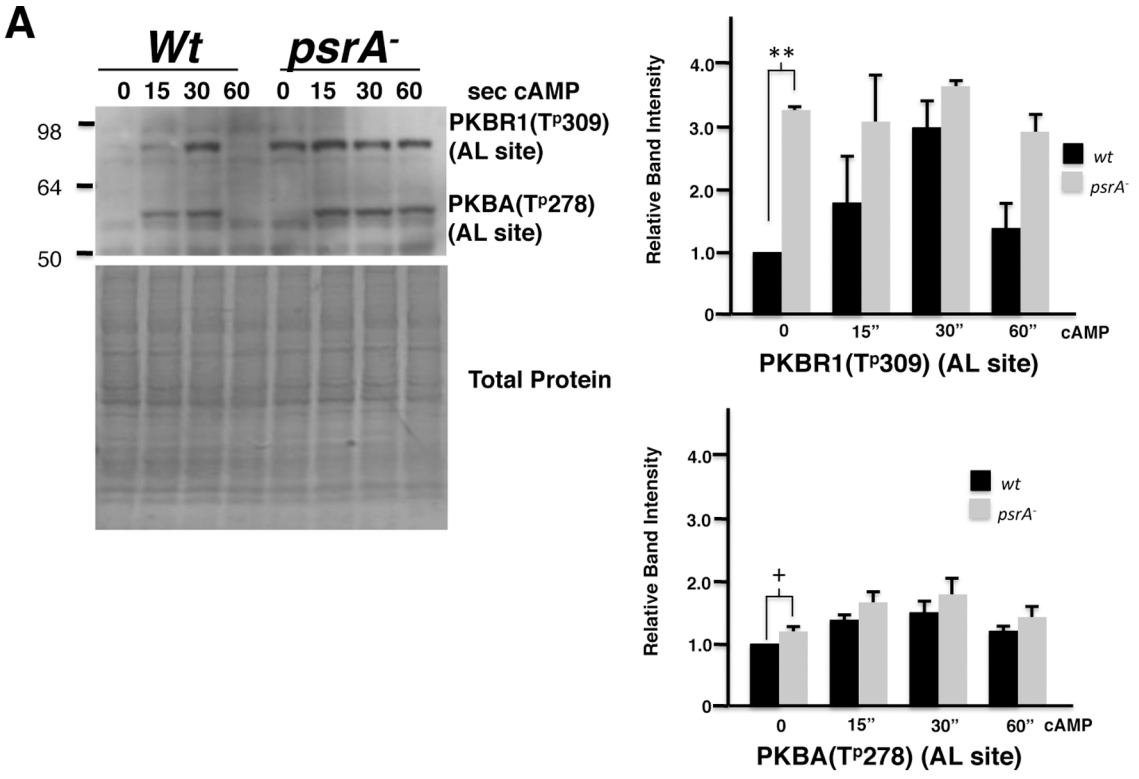
A
Wt
psrA-
0 15 30 60 0 15 30 60 sec cAMP
98
64
50
PKBR1(Tp309) (AL site)
PKBA(Tp278) (AL site)
Total Protein
Relative Band Intensity
4.0
3.0
2.0
1.0
0
**
wt
psrA-
0 15" 30" 60" cAMP
PKBR1(Tp309) (AL site)
+
PKBA(Tp278) (AL site)

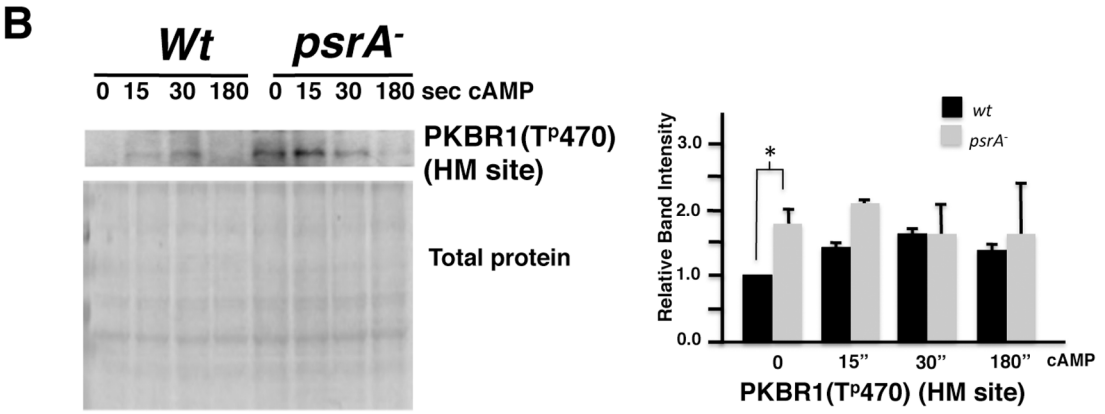
B
Wt
psrA-
0 15 30 180 0 15 30 180 sec cAMP
PKBR1(Tp470) (HM site)
Total protein
Relative Band Intensity
3.0
2.0
1.0
0.0
*
wt
psrA-
0 15" 30" 180" cAMP
PKBR1(Tp470) (HM site)

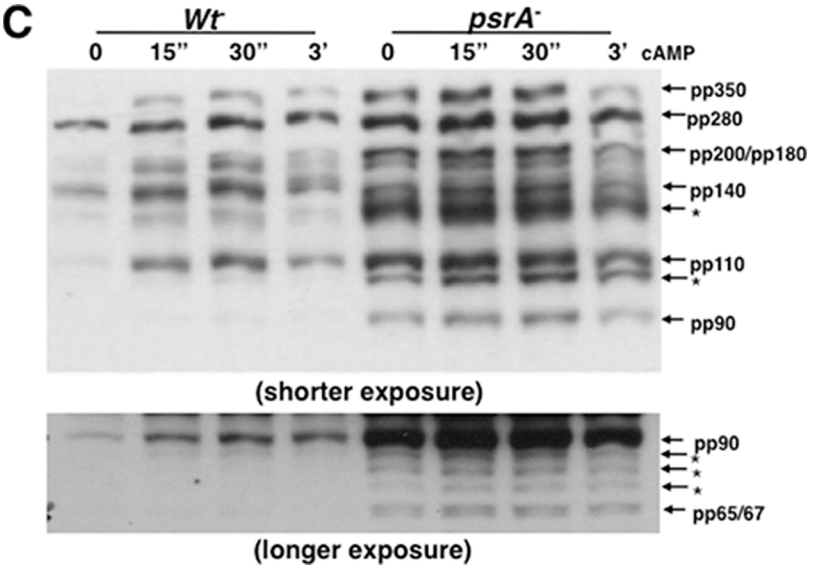
C
Wt
psrA-
0 15" 30" 3' 0 15" 30" 3' cAMP
pp350
pp280
pp200/pp180
pp140
*
pp110
*
pp90
(shorter exposure)
pp90
*
*
*
pp65/67
(longer exposure)

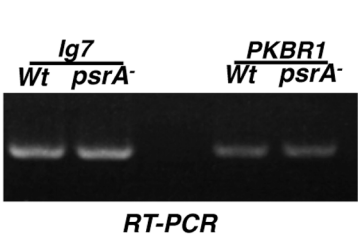
D
lg7
Wt psrA-
PKBR1
Wt psrA-
RT-PCR

wild-type or *psrA*⁻ cells expressing dnGSK3 was observed: no detectable level of active PKBR1 was observed from cells without stimulation, but no statistically significant difference in PKBR1 phosphorylation was observed in response to cAMP stimulation ($^{+}p > 0.05$; Figure 9A). Increased total GSK3 levels of dnGSK3-expressing *rasD*⁻ cells compared with the control cells are shown (Figure 9A). Furthermore, when *rasD*⁻ or *rasC*⁻ cells were treated with LiCl, no significant increase in PKBR1 phosphorylation was observed compared with nontreated cells ($^{+}p > 0.05$; Figure 9, B and C) in contrast to LiCl-treated wild-type and *psrA*⁻ cells, which exhibited higher levels of PKBR1 activation (Figure 8, A and B). Altogether these results suggest that GSK3 affects PKBR1 activity via a RasD- or RasC-dependent mechanism.

DISCUSSION

We report here that B56/PP2A associates with GDP-RasC and GDP-RasD and significantly affects PKB activities in the context of chemotaxis. PP2A function was reported to be essential for chemotaxis by mediating proper regulation of the scaffolding protein Sca1 and Ras proteins (Charest *et al.*, 2010). Currently it is unclear whether B56 or another regulatory B subunit has a role in Sca1-mediated Ras regulation, because no regulatory subunit was identified from the Sca1 protein complex from either unstimulated or stimulated cells (Charest *et al.*, 2010). On receiving a cAMP signal, the PP2A/Sca1/Aimless/GefH complex relocalized to the plasma membrane from the cytosol and thus activated GDP-RasC (Charest *et al.*, 2010). GDP-Ras/B56 may associate with the PP2A/Sca1/Aimless/GefH complex in response to cAMP, which in turn would facilitate GDP-RasC interaction with Aimless/RasGef. On activation of RasC and subsequently PKBs, the Sca1 complex will be phosphorylated and become inactivated by PKBs. For chemotaxing cells to respond to another round of signaling, dephosphorylation of both PKBs and Sca1 complex must occur.

Cells lacking both PKBR1 and PKBA display lower Sca1 phosphorylation and high basal and poststimulus RasC activity. Active RasC will then activate PKBs, which in turn will inhibit Sca1 complex, and thus a negative-feedback loop will be formed (Charest *et al.*, 2010). However, given that activation of PKBR1 and PKBA require cAMP signaling, it is puzzling that basal RasC activity is also aberrantly high in *pkbr1*⁻*/pkba*⁻ double-knockout cells. One possibility is that PKBR1 is not only modulating Sca1/RasC signaling but is also involved in the proper expression of certain genes involved in the regulation of RasC (such as *RasGAP*), considering that PKBR1 can also affect cell differentiation (Meili *et al.*, 2000).

Chemoattractant-mediated activation of specific Ras proteins led to specific downstream events orchestrating directional cell migration. However, previous studies also showed a compensation mechanism between Ras proteins: ablation of RasG increased the level of RasD, but that of RasC showed no such compensation (Bolourani *et al.*, 2010). Thus, expressing high levels of RasD, *rasG*⁻ cells are able to stimulate PKBs. In contrast, lacking RasD, *rasC*⁻ cells are unable to activate PKBs. *rasG*⁻*/rasC*⁻ cells display a significantly lower RasD level compared with that of *rasG*⁻ cells, and thus phosphorylation of PKBs and PKB substrates in *rasG*⁻*/rasC*⁻ is lower than in *rasG*⁻ cells, which is consistent with an earlier study (Srinivasan *et al.*, 2013). In addition, a previous study showed that RasD can form a protein complex including ERK2, PKBA, GRP125, and Filamin (Bandala-Sanchez *et al.*, 2006), indicating a possibility that RasD may mediate association of PP2A/B56 with PKBA. As GTP-RasD/PKBA complex adapts to GDP-RasD/PKBA as a post-cAMP stimulus response, B56/PP2A may join the newly emerging GDP-RasD-PKBA complex and thus inactivate PKBA. Thus, PP2A/B56 could function as a PKB phosphatase similarly to the mammalian PP2A/B56 that dephosphorylates Akt (Rodgers *et al.*, 2011).

The current study also demonstrated that GSK3/RasD is another significant component of PKB inhibitory circuits. Inhibition of GSK3 either with LiCl or expressing dnGSK3 resulted in a significant increase in the level of PKBR1 phosphorylation in wild-type and *psrA*⁻ cells but not in cells lacking RasD or RasC. Interestingly, the dnGSK3-expressing *psrA*⁻ cells but not the wild-type cells expressing dnGSK3 exhibited exaggerated cAMP-mediated PKBA activation in addition to the high PKBR1 activity. Thus either a B56- or a GSK3-mediated suppressive mechanism is sufficient to maintain low PKBA activity, but both mechanisms are necessary for suppressing PKBR1 activity. In addition, we speculate that both PP2A/B56 and GSK3/RasD are likely functioning at the upstream components of PKBs such as Pdk1 or TorC2, but B56/PP2A could directly dephosphorylate PKBA in a RasD-dependent manner.

Consistent with the high PKB activities, the levels of phosphorylation of PKB substrates are also high in *psrA*⁻ cells. Misregulation of Talin and p21-activated kinase A (PAKa) (Chung *et al.*, 2001) would have immediate impact on the cell migration, but other proteins—either previously identified PKB substrates (pp350, pp200/pp180 for GefN, pp140 for GacG, pp110 for GefS/PI5K, pp65/67 for GacQ) or several novel targets reported here—may also participate in the orchestration of the cell migration control.

Regulation of PKBs is a complex event. There seem to exist multiple mechanisms of activation and adaptation that involve multiple Ras proteins, PP2A/B56, and GSK3, either functioning in parallel or cooperatively. Furthermore, feedback inhibition and gene expression circuits are likely implicated. Further investigation is necessary to fully uncover the mechanism of PKB regulation, which will provide novel mechanistic insight on the regulation of PKBs that not only

FIGURE 5: *psrA*⁻ cells exhibited aberrantly high PKBR1 activity and PKB substrate phosphorylation. (A) Compared with *Wt* cells, *psrA*⁻ cells exhibited an abnormally high basal level of phosphorylated PKBR1 at the AL site, which persisted in response to cAMP stimulation. The levels of basal PKBR1 phosphorylation in *psrA*⁻ cells are consistently higher (approximately three times) than those of wild-type cells (three independent experiments; **, $p < 0.01$). The levels of basal PKBA phosphorylation of *Wt* and *psrA*⁻ cells showed no statistically significant difference ($^{+}$, $p > 0.05$). PKBA also displayed persistent activation in response to cAMP stimulation in *psrA*⁻ cells. The phospho-PKB levels were normalized to Coomassie-stained total proteins. (B) *psrA*⁻ cells also displayed aberrantly higher basal and poststimulus levels of phosphorylated PKBR1 at the HM site in response to cAMP stimulation. (C) Phosphorylation levels of PKB substrates in *psrA*⁻ and *Wt* cells were detected using the anti–phospho Akt substrate antibody. *psrA*⁻ cells displayed significantly increased basal level of phosphoproteins. Some of these proteins seem to be *psrA*⁻ cell specific as marked (*), and the others could be assigned to the previously reported PKBR1/PKBA substrate proteins (pp350, pp280 for TalinB, pp200/pp180 for GefN, pp140 for GacG/PakA, pp110 for GefS/PI5K, pp65/67 for GacQ; Cai *et al.*, 2010). (D) Comparable levels of *PKBR1* messages were detected from wild-type and *psrA*⁻ cells by RT-PCR. *Ig7* messages were shown as loading control. Error bars represent SD.

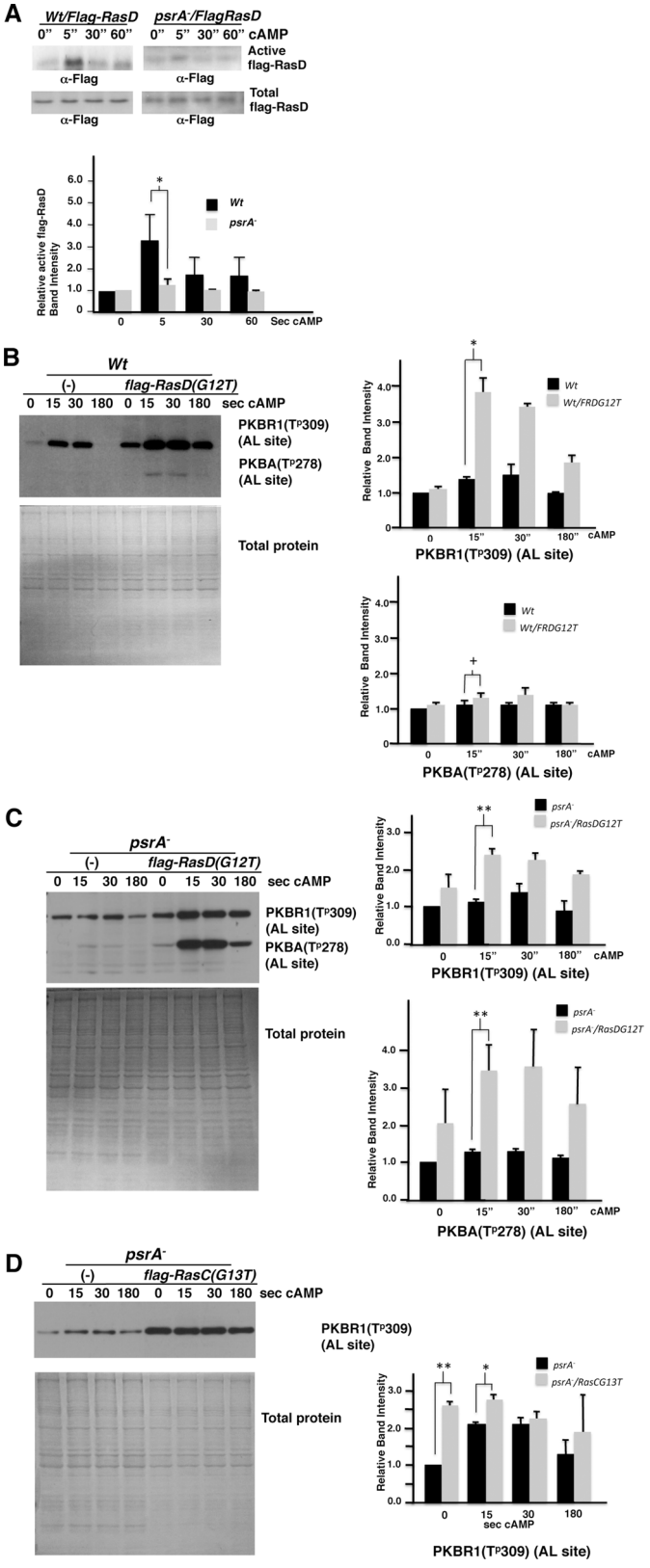

FIGURE 6: Introducing constitutively active RasD increased PKBR1 and PKBA activities in *psrA*⁻ cells. (A) Wild-type and *psrA*⁻ cells expressing Flag-RasD proteins were stimulated with cAMP, and the total amount of Flag-RasD was normalized. Then the active Flag-RasD protein levels were determined using GST-RBD followed by anti-Flag Western blotting. Relative active RasD levels were quantitated by normalizing the total Flag-RasD amount in the input. (B) *Wt* cells expressing Flag-RasD(G12T) also exhibited augmented basal and poststimulus phosphorylation of PKBR1 (three independent experiments, 2.5 times higher 15-s poststimulus level; *, $p < 0.05$). *Wt* cells expressing Flag-RasD(G12T) showed no significant changes in the levels of PKBA phosphorylation (+, $p > 0.05$). The phospho-PKBR1 levels were normalized to Coomassie-stained total proteins. (C) Introducing the constitutively active Flag-RasD(G12T) in *psrA*⁻ cells resulted in even higher basal and poststimulus PKBR1 phosphorylation (three independent experiments, approximately twofold higher at 15-s poststimulation; **, $p < 0.01$). Significantly higher levels of poststimulus phosphorylation of PKBA were observed in Flag-RasD(G12T)–expressing *psrA*⁻ cells (**, $p < 0.01$). The phospho-PKBR1 levels were normalized to Coomassie-stained total proteins. (D) *psrA*⁻ cells expressing Flag-RasC(G13T), as previously reported (Cai *et al.*, 2010), showed increases in basal and poststimulus phosphorylation of PKBR1 (three independent experiments, ~2.5-fold higher basal level; **, $p < 0.01$; 35% higher 15-s poststimulation; *, $p < 0.05$), but no such change was observed for PKBA. The phospho-PKBR1 levels were normalized to Coomassie-stained total proteins. Error bars represent SD.

regulate chemotaxis but other F-actin remodeling–mediated events such as phagocytosis and macropinocytosis.

MATERIALS AND METHODS

Cell culture

Ax3, *psrA*⁻, *gsk3*⁻, *rasC*⁻, *rasD*⁻, *psrA*⁻/*FlagRasD(G12T)*, *psrA*⁻/*FlagRasCG13T*, *psrA*⁻/*dnGSK3*, *Wt/dnGSK3*, and cells were grown with axenic medium (14.3 g peptone 3 [Difco, Detroit, MI], 7.15 g yeast extract [Oxoid, Hampshire, United Kingdom], 15.4 g glucose [Fisher Scientific, Waltham, MA], 0.525 g $Na_2HPO_4{\cdot}7H_2O$, 0.48 g KH_2PO_4, 0.53 g $Na_2HPO_4{\cdot}7H_2O$ in 1 l of water, pH 6.5–6.9). The medium was complemented with 5 mg/ml of blasticidin (InvivoGene, San Diego, CA) for *psrA*⁻, *rasC*⁻, *rasD*⁻, and *gsk3*⁻ strains. In addition, for *gsk3*⁻ cells, 25 mg/ml of thymidine (Arcos Organics/Fisher Scientific, Waltham, MA) was added to the medium. For strains overexpressing FlagRasC, FlagRasD, FlagRasC(G13T), FlagRasD(G12T), or dnGSK3, 20 μg/ml of G418 (Gibco) was used as a selective agent for the medium.

Recombinant ras proteins

Ras mutant constructs were generated by using the QuikChange Site-Directed Mutagenesis kit (Stratagene/NEB, Ipswich, MA). Each construct was fully sequenced and subcloned into an *E. coli* expression vector (pGEX-4T-2) in which the GST-encoding sequence was substituted with a Flag-tag sequence, and the recombinant proteins were immunopurified by anti-Flag antibody and eluted with Flag peptide for various binding assays.

Pull-down assays

To examine Ras activation in response to cAMP stimulation, log-phase vegetative cells, either *Wt*, *psrA*⁻, or various Ras mutant–expressing cells, were starved for 1 h and stimulated with 50 nM cAMP at 6 min intervals for 4 h at room temperature at a concentration of 20×10^6 cells/ml in DB buffer (2 mM $MgCl_2$, 0.2 mM $CaCl_2$, 7.4 mM NaH_2PO_4, 4mM Na_2HPO_4). Aggregation-competent cells were washed once with ice-cold DB buffer and treated with 5 mM caffeine at room temperature for 20 min at a concentration of 20×10^6 cells/ml. Following treatment, cells were washed with ice-cold DB buffer once, resuspended with 5 ml of DB buffer, and shaken

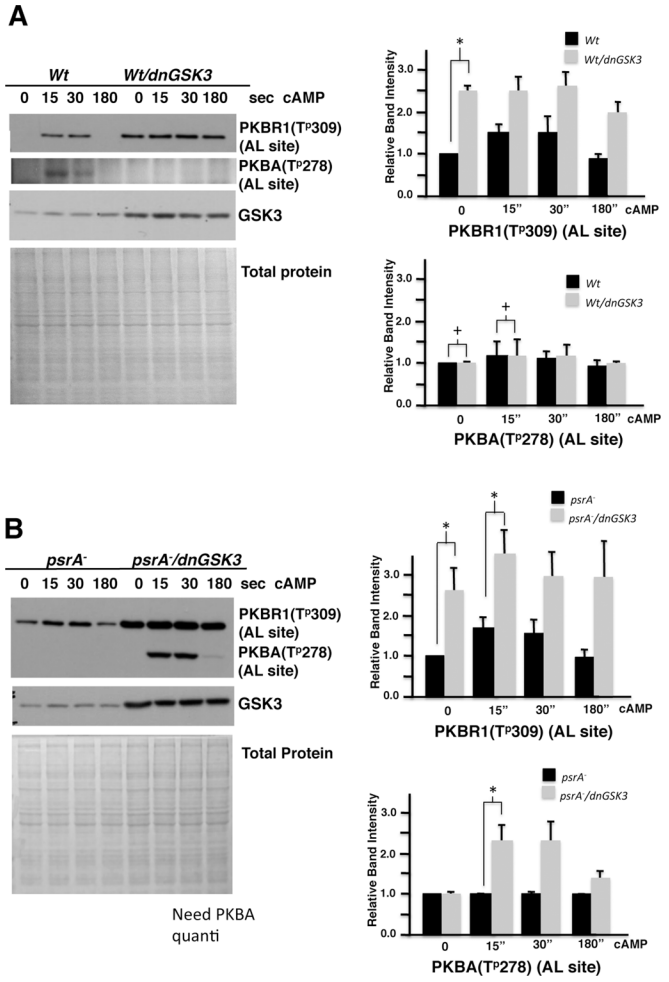

FIGURE 7: Introducing dnGSK3 increased PKBA and PKBR1 activities in *psrA*⁻ cells. (A) *Wt* cells expressing the dnGSK3 exhibited higher levels of basal phosphorylation of PKBR1, which persisted upon cAMP stimulation (*, $p < 0.05$). No such significant changes were observed for PKBA phosphorylation (+, $p > 0.05$). The phospho-PKBR1 levels were normalized to Coomassie-stained total proteins. (B) *psrA*⁻ expressing the dnGSK3 showed high basal and persistent poststimulus phosphorylation of PKBR1 (three independent experiments, ~2.5-fold higher basal and twofold increase in 15-s poststimulus levels; +, $p < 0.05$) and exaggerated poststimulus phosphorylation of PKBA. The phospho-PKBs levels were normalized to Coomassie-stained total proteins. Error bars represent SD.

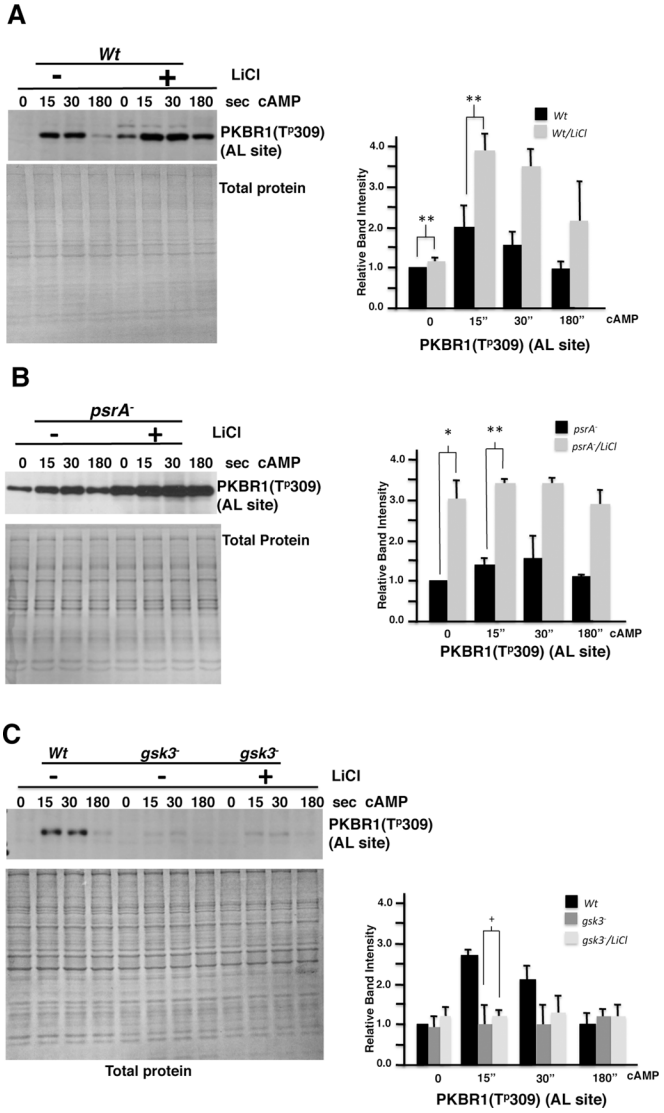

FIGURE 8: Cells treated with LiCl exhibited increased PKBR1 activation. (A) *Wt* cells treated with GSK3 inhibitor, LiCl, showed increased poststimulus phosphorylation levels of PKBR1 compared with untreated cells: *Wt* cells treated with LiCl exhibited ~30% increase in the basal level of PKBR1 activity and an approximately twofold increase in the level of PKBR1 phosphorylation after cAMP stimulation compared with nontreated cells (**, $p < 0.01$). The phospho-PKBR1 levels were normalized to Coomassie-stained total proteins. (B) LiCl-treated *psrA*⁻ cells exhibited even higher levels of basal phosphorylation of PKBR1 compared with nontreated *psrA*⁻ cells ($p < 0.05$). At 5-s poststimulus, the phosphorylation level of LiCl-treated *psrA*⁻ cells was consistently higher than the control (**, $p < 0.01$). The phospho-PKBR1 levels were normalized to Coomassie-stained total proteins. (C) Unlike *Wt* or *psrA*⁻ cells, cells lacking GSK3 showed no significant differences in PKBR1 phosphorylation in response to LiCl treatment (+, $p > 0.05$). The phospho-PKBR1 levels were normalized to Coomassie-stained total proteins. Error bars represent SD.

for 2 min at room temperature. Then cells were stimulated with 10 μM cAMP and immediately lysed with TTG buffer (20 mM Tris-Base, 150 mM NaCl, 0.1% Triton-X, 20% glycerol, 1 mM EDTA, 0.1% 2-mercaptoethanol, and protease inhibitor cocktail from Roche) at 5, 30, 60, and 90 s. Alternatively, aggregation-competent Flag-RasD– or Flag-RasC–expressing wild-type cells were incubated further with and without 1 mM GTP-γ-S for 20 min on ice, lysed with TTG buffer, and used for GST-RBD or GST-B56 pull-down assays.

The activated forms of RasD and RasG were purified using recombinant GST- RBD from mammalian Raf1 (GST-RBDRaf1) and the activated form of RasC was purified using recombinant GST-RBD from *S. pombe* Byr2 (GST-RBDByr2). Cell extracts were mixed with 4 μg of either purified GST-RBD-Raf1 or purified GST-RBD-Byr2 and incubated at 4°C for 90 min. Samples were then washed three times using TTG buffer. SDS-containing sample buffer was then added to the pull-down complexes; samples were analyzed using a Tris-glycine–SDS–polyacrylamide gel, and the levels of active Ras were detected by Western blot using anti-Pan-Ras antibody (Calbiochem).

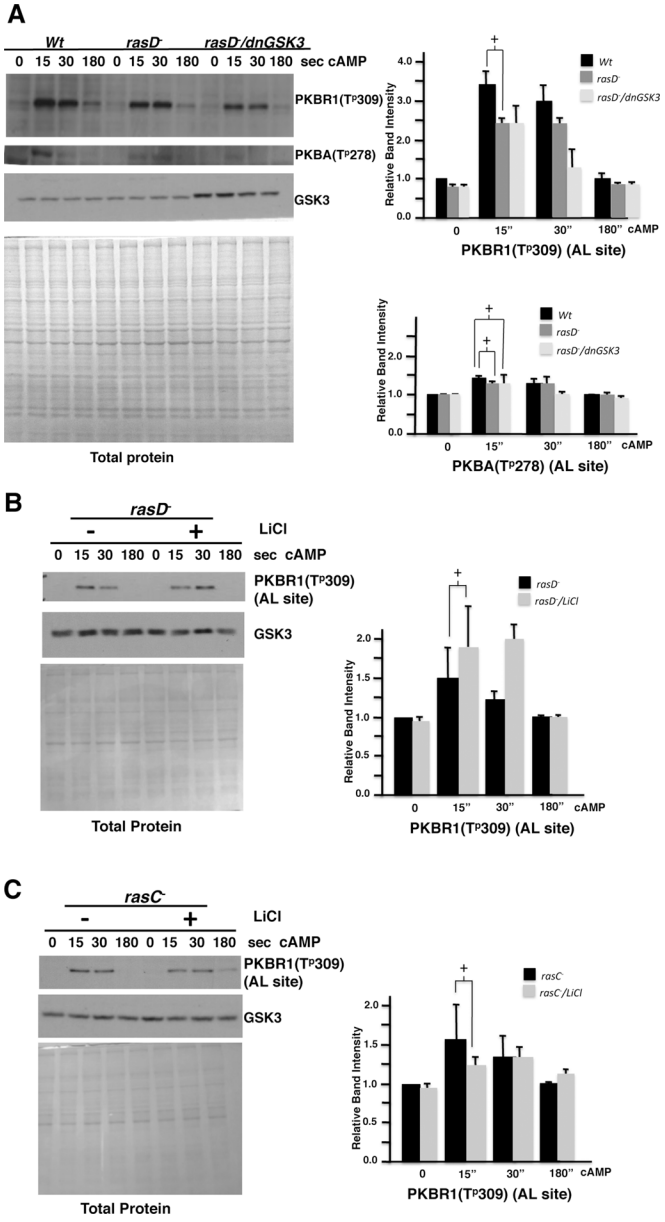

FIGURE 9: dnGSK3- and LiCl-mediated regulation of phosphorylation of PKBR1 is Ras dependent. (A) *rasD*$^-$ cells showed normal basal and comparable poststimulus phosphorylation of PKBR1. *rasD*$^-$ cells expressing dnGSK3 displayed no significant increase in the basal phosphorylation levels of PKBR1 and PKBA. In response to cAMP stimulation, *rasD*$^-$ cells expressing dnGSK3 exhibited comparable levels of PKBR1 phosphorylation compared with *rasD*$^-$ cells ($^+$, $p > 0.05$). The phospho-PKBR1 levels were normalized to Coomassie-stained total proteins. (B and C) *rasD*$^-$ and *rasC*$^-$ cells treated with LiCl showed no significant changes in the basal and poststimulus phosphorylation levels of PKBR1 ($^+$, $p > 0.05$). The phospho-PKBR1 levels were normalized to Coomassie-stained total proteins. Error bars represent SD.

B56-bound Ras proteins were similarly detected by GST-B56 pull-down assay as previously described (Lee *et al.*, 2008).

Chemotaxis and random motility assays

Log-phase cells were starved at a concentration of 20×10^6 cells/ml in DB buffer for 1 h; this was followed by stimulation with 50 nM cAMP every 6 min for a total of 4 h at room temperature. Aggregation-competent cells were plated at a density of 3×10^4 cells/cm^2 on a 35-mm tissue culture dish cover (Falcon 353001; Becton Dickinson) and left to settle down for 5–10 min at room temperature. For examination of the chemotactic response, cells were exposed with a Schmazu micromanipulator to a glass capillary needle filled with either 10 μM cAMP or 0.1 mM folic acid solution. For maintaining the external chemotactic gradient, the capillary needle containing chemoattractant was connected to an Eppendorf FemtoJet at an injection pressure of 20 hPa. A time-lapse video recording using OpenLab Software was used to follow the cell movement at 1-min intervals. For a random motility analysis, aggregation-competent cells were plated as previously described, and no source of external cAMP was used. Chemotactic indices and the speed were analyzed as previously described (Veeranki *et al.*, 2008).

Determining PKBR1 activation in response to cAMP stimulation

For examination of PKBR1 activation, aggregation-competent cells were washed once with ice-cold DB buffer and treated with 5 mM caffeine at room temperature for 20 min. After the treatment, cells were washed twice with ice-cold PM buffer (5 mM Na_2HPO_4, 5 mM KH_2PO_4, 2 mM $MgSO_4$) and resuspended at 20×10^6 cells/ml in PM buffer; this was followed by shaking for 2 min at room temperature, and then cells were stimulated with 1 μM cAMP, which was followed by lysis with TTG buffer at 15, 30, and 180 s. PKBR1 phosphorylation was detected with Western blotting using phospho-PKC antibody (Cell Signaling 190D10) as previously described by Cai and colleagues (2010). To detect the phosphorylation of PKBR1 substrates containing the motif R-x-R-x-x-S/T-x-x, Western blot using anti–phospho Akt Substrate (Cell Signaling) was done as previously described by Kamimura *et al.* (2008).

To analyze PKBR1 activation in the presence of LiCl, aggregation-competent cells were treated with 50 mM LiCl for 1 h at room temperature with shaking. Cells were then washed once with ice-cold DB; this was followed by caffeine treatment and stimulation with 1 μM cAMP as previously described. The IC_{50} of LiCl on GSK3 activity is 4 mM by using GSK3-specific peptide substrate (L. W. Kim, unpublished data) as reported previously (Ryves *et al.*, 1998). A measure of 50 mM LiCl is known to be sufficient for the near-complete suppression of GSK3 activity (L. W. Kim, unpublished data, Ryves *et al.*, 1998).

ACKNOWLEDGMENTS

This work was supported by a National Institutes of Health (NIH) SC1 grant (CA143958) from the National Cancer Institute to L.W.K. M.R.P. and B.C. were recipients of MBRS RISE fellowships from the NIH. We appreciate years of excellent service from the *Dictyostelium* Stock Center. *pkbA*$^-$ and *pkbr1*$^-$ cells were from the *Dictyostelium* Stock Center. We thank Alan Kimmel (NIH) for his invaluable comments on the manuscript.

REFERENCES

Bandala-Sanchez E, Annesley SJ, Fisher PR (2006). A phototaxis signalling complex in *Dictyostelium discoideum*. Eur J Cell Biol 85, 1099–1106.

Bolourani P, Spiegelman G, Weeks G (2010). Ras proteins have multiple functions in vegetative cells of *Dictyostelium*. Eukaryot Cell 9, 1728–1733.

Cai H, Das S, Kamimura Y, Long Y, Parent C, Devreotes P (2010). Ras mediated activation of the TORC2-PKB pathway is critical for chemotaxis. J Cell Biol 190, 233–245.

Charest P, Shen Z, Lakoduk A, Sasaki A, Briggs S, Firtel R (2010). A Ras signaling complex controls the RasC-TORC2 pathway and directed cell migration. Dev Cell 18, 737–749.

Chattwood A, Bolourani P, Weeks G (2014). RasG signaling is important for optimal folate chemotaxis in *Dictyostelium*. BMC Cell Biology 15, 13.
Chung CY, Potikyan G, Firtel R (2001). Control of cell polarity and chemotaxis by Akt/PKB and PI3 kinase through the regulation of PAKa. Mol Cell 7, 937–947.
Funamoto S, Meili R, Lee S, Parry L, Firtel RA (2002). Spatial and temporal regulation of 3-phosphoinositides by PI 3-kinase and PTEN mediates chemotaxis. Cell 109, 611–623.
Iijima M, Devreotes P (2002). Tumor suppressor PTEN mediates sensing of chemoattractant gradients. Cell 109, 599–610.
Insall RH, Borleis J, Devreotes PN (1996). The aimless RasGEF is required for processing of chemotactic signals through G-protein-coupled receptors in *Dictyostelium*. Curr Biol 6, 719–729.
Janetopoulos C, Jin T, Devreotes P (2001). Receptor-mediated activation of heterotrimeric G-proteins in living cells. Science 291, 2408–2411.
Jeon TJ, Lee DJ, Lee S, Weeks G, Firtel RA (2007a). Regulation of Rap1 activity by RapGAP1 controls cell adhesion at the front of chemotaxing cells. J Cell Biol 179, 833–843.
Jeon TJ, Lee DJ, Merlot S, Weeks G, Firtel RA (2007b). Rap1 controls cell adhesion and cell motility through the regulation of myosin II. J Cell Biol 176, 1021–1033.
Kae H, Kortholt A, Rehmann H, Insall RH, Van Haastert PJ (2007). Cyclic AMP signaling in *Dictyostelium*: G-proteins activate separate Ras pathways using specific RasGEFs. EMBO Rep 8, 477–482.
Kamimura Y, Devreotes PN (2010). Phosphoinositide-dependent protein kinase (PDK) activity regulates phosphatidylinositol 3,4,5-triphosphate-dependent and –independent protein kinase B activation and chemotaxis. J Biol Chem 285, 7938–7946.
Kamimura Y, Xiong Y, Iglesias PA, Hoeller O, Bolourani P, Devreotes PN (2008). PIP3-independent activation of TorC2 and PKB at the cell's leading edge mediates chemotaxis. Curr Biol 18, 1034–1043.
Khosla M, Spiegelman GB, Insall R, Weeks G (2000). Functional overlap of the *Dictyostelium* RasG, RasD and RasB proteins. J Cell Sci 113, 1427–1434.
Kim L, Brzostowski J, Majithia A, Lee N, McMains V, Kimmel AR (2011). Combinatorial cell-specific regulation of GSK3 directs cell differentiation and polarity in *Dictyostelium*. Development 138, 421–430.
Kim L, Harwood A, Kimmel AR (2002). Receptor-dependent and tyrosine phosphatase-mediated inhibition of GSK3 regulates cell fate choice. Dev Cell 3, 523–532.
King JS, Teo R, Ryves J, Reddy JV, Peters O, Orabi B, Hoeller O, Williams RSB, Adrian J, Harwood AJ (2009). The mood stabiliser lithium suppresses PIP3 signalling in *Dictyostelium* and human cells. Dis Model Mech 2, 306–312.
Kölsh V, Shen V, Lee S, Plak K, Lotfi P, Chang J, Charest P, Lacal-Romero J, Jeon T, Kortholt A, *et al*. (2012). Daydreamer, a Ras effector and GSK3 substrate, is important for directional sensing and cell motility. Cell Dev Biol 24, 100–114.
Kortholt A, Rehmann H, Kae H, Bosgraaf L, Keizer-Gunnink I (2006). Characterization of the GbpD-activated Rap1 pathway regulating adhesion and cell polarity in *Dictyostelium discoideum*. J Biol Chem 281, 23367–23376.
Kortholt A, van Haastert PJ (2008). Highlighting the role of Ras and Rap during *Dictyostelium* chemotaxis. Cell Signal 20, 1415–1422.
Lee NS, Veeranki S, Kim B, Kim L (2008). The function of PP2A/B56 in non-metazoan multicellular development. Differentiation 76, 1104–1110.
Lee S, Comer FI, Sasaki A, McLeod IX, Duong Y, Okumura K, Yates JR. III, Parent CA, Firtel RA (2005). TOR complex 2 integrates cell movement during chemotaxis and signal relay in *Dictyostelium*. Mol Biol Cell 16, 4572–4583.
Letourneux C, Rocher G, Porteu F (2006). B56-containing PP2A dephosphorylate ERK and their activity is controlled by the early gene IEX-1 and ERK. EMBO J 25, 727–738.
Liao XH, Buggey J, Kimmel AR (2010). Chemotactic activation of *Dictyostelium* AGC-family kinases AKT and PKBR1 requires separate but coordinated functions of PDK1 and TORC2. J Cell Sci 123, 983–992.
Meili R, Ellsworth C, Firtel RA (2000). A novel Akt/PKB-related kinase is essential for morphogenesis in *Dictyostelium*. Curr Biol 10, 708–717.
Meili R, Ellsworth C, Lee S, Reddy TB, Ma H, Firtel RA (1999). Chemoattractant-mediated transient activation and membrane localization of Akt/PKB is required for efficient chemotaxis to cAMP in *Dictyostelium*. EMBO J 18, 2092–2105.
Mondal S, Bakthavatsalam D, Steimle P, Gassen B, Rivero F, Noegel AA (2008). Linking Ras to myosin function: RasGEF Q, a *Dictyostelium* exchange factor for RasB, affects myosin II functions. J Cell Biol 181, 747–760.
Padmanabhan S, Mukhopadhyay A, Narasimhan SD, Tesz G, Czech MP, Tissenbaum HA (2009). A PP2A regulatory subunit regulates *C. elegans* insulin/IGF-1 signaling by modulating Akt-1 phosphorylation. Cell 136, 939–951.
Rocher G, Letourneux C, Lenormand P, Porteu F (2007). Inhibition of B56-containing protein phosphatase 2As by the early response gene IEX-1 leads to control of Akt activity. J Biol Chem 282, 5468–5477.
Rodgers JT, Vogel R, Puigserver P (2011). Clk2 and B56b mediate insulin-regulated assembly of the PP2A phosphatase holoenzyme complex on Akt. Mol Cell 41, 471–479.
Ryves WJ, Fryer L, Dale T, Harwood AJ (1998). An assay for glycogen synthase kinase 3 (GSK-3) for use in crude cell extracts. Anal Biochem 264, 124–127.
Srinivasan K, Wright GA, Hames N, Housman M, Roberts A, Aufderheide KJ, Janetopoulos C (2013). Delineating the core regulatory elements crucial for directed cell migration by examining folic-acid-mediated responses. J Cell Sci 126, 221–233.
Sun T, Kim B, Kim L (2013). Glycogen synthase kinase 3 influences cell motility and chemotaxis by regulating PI3K membrane localization in *Dictyostelium*. Dev Growth Differ 55, 723–734.
Swaney KF, Huang CH, Devreotes PN (2010). Eukaryotic chemotaxis: a network of signaling pathways controls motility, directional sensing, and polarity. Annu Rev Biophys 39, 265–289.
Teo R, Lewis K, Forde JE, Ryves WJ, Reddy JV, Rogers BJ, Harwood AJ (2010). Glycogen synthase kinase 3 is required for efficient *Dictyostelium* chemotaxis. Mol Biol Cell 21, 2788–2796.
Veeranki S, Kim B, Kim L (2008). The GPI-anchored superoxide dismutase SodC is essential for regulating basal Ras activity and for chemotaxis of *Dictyostelium discoideum*. J Cell Sci 121, 3099–3108.
Weeks G (2000). Signalling molecules involved in cellular differentiation during *Dictyostelium* morphogenesis. Curr Opin Microbiol 3, 625–630.
Xu X, Meier-Schellersheim M, Jiao X, Nelson LE, Jin T (2005). Quantitative imaging of single live cells reveals spatiotemporal dynamics of multistep signaling events of chemoattractant gradient sensing in *Dictyostelium*. Mol Biol Cell 16, 676–688.